

Article

Electrochemical and Surface Analysis of 2-Phenylimidazole Adsorbed on Copper from Chloride Solution

Matjaž Finšgar ^{1,*} and Klodian Xhanari ^{1,2}

¹ Faculty of Chemistry and Chemical Engineering, University of Maribor, Smetanova Ulica 17, Maribor 2000, Slovenia

² Faculty of Natural Sciences, University of Tirana, Boulevard “Zogu I”, Tirana 1001, Albania; klodian.xhanari@fshn.edu.al

* Correspondence: matjaz.finsgar@um.si; Tel.: +386-2-2294-447

Received: 16 May 2018; Accepted: 2 July 2018; Published: 3 July 2018



Abstract: The electroanalytical and surface characterization of copper immersed in 3 wt.% NaCl solution containing 1 mM of 2-phenylimidazole (2PhI) is presented. It was proven that 2PhI can be employed as corrosion inhibitor for copper using various electrochemical analyses, such as cyclic voltammetry, chronopotentiometry, electrochemical impedance spectroscopy, and potentiodynamic curve measurements. The adsorption of 2PhI on copper was further analyzed by 3D-profilometry, attenuated total reflectance Fourier transform infrared spectroscopy, contact angle measurements, and scanning electron microscopy equipped with an energy dispersive X-ray spectrometer. This system was therefore comprehensively described by various analytical approaches.

Keywords: corrosion inhibitor; copper; electrochemical impedance spectroscopy (EIS); cyclic voltammetry; attenuated total reflectance Fourier transform infrared (ATR-FTIR)

1. Introduction

Corrosion and corrosion-prevention-related costs represent a significant portion of the gross domestic product (GDP) of the developed countries, amounting to 3–5% thereof, or possibly even higher [1–3]. Corrosion cannot be completely prevented, but it can be mitigated to a certain degree by means of the right methods. The selection of a method is closely connected to the combination of the material and the corrosive environment. The use of corrosion inhibitors is convenient in the case of closed systems [4], however a closed system is not mandatory. Several organic or inorganic chemical compounds can act as corrosion inhibitors by adsorption on the surface of the metals. The adsorbed inhibitor layer formed starts to mitigate corrosion. This will then result in a lower corrosion rate. Corrosion inhibitors are dissolved in a corrosive medium at very low concentrations. Numerous studies have been performed at 1 mM concentration of corrosion inhibitor [5–12]. Copper is one of the most important metals among the nonferrous materials; however, it suffers from corrosion in chloride-containing media.

A detailed electrochemical impedance spectroscopy can be applied to reveal the properties of surface layers and the mechanism of the corrosion inhibitor action. Furthermore, spectroscopic analysis is also beneficial as it can support the analytical results obtained by means of electrochemistry and provides deeper insight into the corrosion inhibitor system. For this reason, a combination of electrochemical analysis, spectroscopic analysis, and surface characterization was employed herein to fully describe the system.

Herein, for the first time 2-phenylimidazole (2PhI) was shown to be an effective corrosion inhibitor for copper in chloride media. Imidazole compounds are attractive in the field of corrosion inhibitor

research as they contain nitrogen atoms in five-membered ring, which can work as binding centers in the adsorption process. Adsorption is the first condition for a specific compound to be considered a corrosion inhibitor. Several other azole compounds have been previously reported as effective corrosion inhibitors for copper in chloride solutions. Previously, we demonstrated for the first time that 4-methyl-2-phenylimidazole (MePhI) [6,13] and 2-aminobenzimidazole [5] are effective corrosion inhibitors for copper in 3 wt.% NaCl solution. Since MePhI is an effective corrosion inhibitor, a question that arises is whether the methyl group in that compound is crucial for the adsorption process (compare the structures in Figure 1). On that basis, 2PhI was selected for the research presented herein.

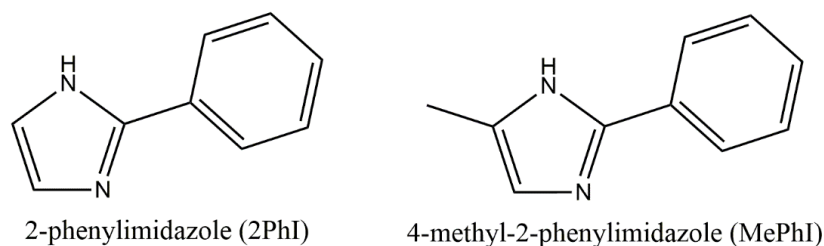


Figure 1. The structure of the corrosion inhibitor tested (2PhI) compared with MePhI.

A relatively high chloride content (3 wt.% NaCl) was employed in this case in order to study the worst-case scenario. However, copper is usually exposed to corrosive environments with lower chloride content. Various analytical techniques were employed in this study. First, weight loss tests were performed followed by various electrochemical techniques including cyclic voltammetry (CV), chronopotentiometry, electrochemical impedance spectroscopy (EIS), and potentiodynamic curve measurements. The adsorption of 2PhI was proved by attenuated total reflectance Fourier transform infrared (ATR-FTIR) spectroscopy analysis. The hydrophobic nature of the inhibited copper samples was studied by contact angle measurements. Finally, using 3D-profilometry and field emission scanning electron microscopy (FE-SEM) the surface topography and morphology of the 2PhI-inhibited copper samples were studied.

Hitherto, to the best of our knowledge, 2PhI has never before been tested as a corrosion inhibitor for any metallic material and in any electrolyte.

2. Materials and Methods

2PhI with a purity of 98 wt.% was supplied by Sigma Aldrich (St. Louis, MO, USA), while copper with a purity of 99.999% was obtained from Goodfellow (Cambridge, UK). The same solution and sample preparation procedure was used as reported previously [5]. Immersion tests, all the electrochemical measurements, as well as surface characterization (including ATR-FTIR, 3D-profilometry, contact angle and FE-SEM analyses) were performed in the same manner as explained in detail in [5,7,9]. For the electrochemical measurements Gamry 600TM instrument (Warminster, PA, USA) was employed. The CV spectra were recorded after 1 h of immersion. EIS measurements were performed after 5, 10, 30, 50, and 100 h of immersion, while the potentiodynamic (PD) curves were obtained after 100 h of immersion. A potential scan rate of 20 mV s⁻¹ was employed to obtain the CV spectra in the potential range from -0.800 V to 1.000 V vs. the saturated calomel electrode (SCE). The EIS spectra were recorded in the frequency range from 1 MHz to 5 mHz with 10 points per decade and 10 mV (peak to peak) of the excitation signal. Finally, for the PD curve the measurements started at -0.250 V vs. E_{oc} with a potential scan rate of 0.1 mV s⁻¹ going in the anodic direction. Surface characterization has been performed on 2PhI-treated samples after 31 days of immersion. Grubbs' test was employed to check for potential outliers, but none were detected [14]. All the experiments were performed at 25 °C.

3. Results and Discussion

In order to show the influence of the 2PhI on the corrosion susceptibility of the copper samples immersed in 3 wt.% NaCl solution three different concentrations, i.e., 0.1, 0.5 and 1.0 mM were tested after 100 h of immersion, using EIS and PD curve measurements. These techniques provide fast and reliable results. The respective Bode plots and PD curve measurements for different concentrations of 2PhI added are presented in Figure 2. The corrosion resistance of the copper samples immersed in 3 wt.% NaCl solution increased with increasing inhibitor concentration as the absolute impedance values at low frequency provide an estimation of the polarization resistance. This increase is nonsignificant when increasing the concentration of 2PhI from 0.1 to 0.5 mM, while a strong increase of the corrosion resistance (about two orders of magnitude) was observed for Cu samples immersed in 3 wt.% NaCl containing 1 mM 2PhI (Figure 2a). Moreover, the PD curves are transferred to the lower current densities (especially the anodic part) for 1 mM concentration (Figure 2b). Due to the most significant corrosion inhibition effect of the 1 mM concentration and since this concentration was employed previously [5–12] (which will allow comparison of the results), we have employed only 1 mM concentration for the detailed corrosion study that follows below.

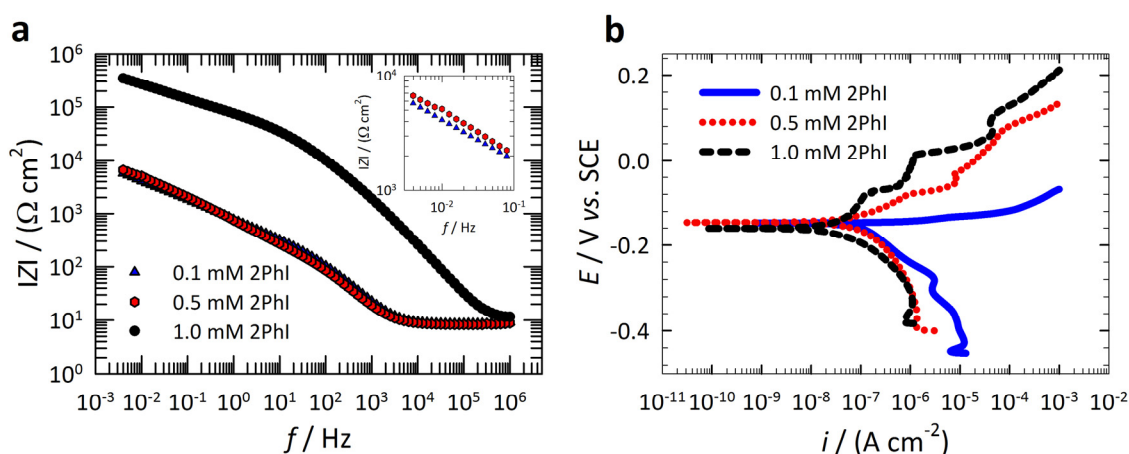


Figure 2. (a) Bode plots and (b) PD curve measurements for Cu samples after 100 h immersion in 3 wt.% NaCl solution containing 0.1, 0.5 and 1.0 mM 2PhI.

3.1. Immersion Tests

After 31 days of immersion in 3 wt.% NaCl solution containing 1 mM 2PhI the copper samples showed mass gain probably due to the inability of the treatment procedure to clean the corroded surface. Moreover, mass gain also indicates corrosion inhibition effect of 2PhI.

3.2. Cyclic Voltammetry (CV) Measurements

The CV curve of the copper sample immersed for 1 h in 3 wt.% NaCl solution containing 1 mM 2PhI is presented in Figure 3. In addition, the cyclic voltammogram of the noninhibited copper samples under the same conditions, reported previously [5], is also given (Figure 3). A potential sweep rate of 20 mV s^{-1} was used to perform both CV experiments.

We have previously reported that in the CV voltammogram of a noninhibited copper sample two anodic peaks (denoted as A_1 and A_2) at 0.342 V and 0.503 V vs. SCE, respectively, and one cathodic peak (denoted as K_1) at -0.460 V vs. SCE were detected [5]. In addition, a small reactivation peak (denoted as A_r) was detected at 0.091 V vs. SCE [5].

The first anodic peak, A_1 , represents the oxidation of Cu to Cu(I). This oxidation occurs first by the electrochemical formation of CuCl_{ads} film on the copper surface. A chemical reaction follows between CuCl and Cl^- and CuCl_2^- complex is formed [6,10]. The second anodic peak represents the

electrochemical oxidation of Cu(I) to Cu(II) [6,10,12,15]. Therefore, the oxidation of copper in chloride solutions follows an electrochemical–chemical–electrochemical mechanism, which is described in more detail in [6,10,12,15]. However, Kologo et al. [16] proposed an electrochemical–electrochemical mechanism for the oxidation of copper in chloride solutions, related to the direct oxidation of the CuCl_{ads} film to form Cu^{2+} according to Equation (1).



The current plateau observed for potentials more positive than the potential of the A_2 peak is related to the equilibrium between the formation of CuCl film on the copper surface and the dissolution of CuCl_2^{-} complex [6,10,12,15,17].

The reason for the formation of an anodic reactivation peak, A_r , observed in Figure 3 was explained previously [12]. The only cathodic peak, designated as K_1 , is connected with the reduction of Cu(I) to Cu [6,12]. The Cu^{2+} species are not reduced because due to their solubility they leave the electrode's surface and diffuse into the solution [15,18].

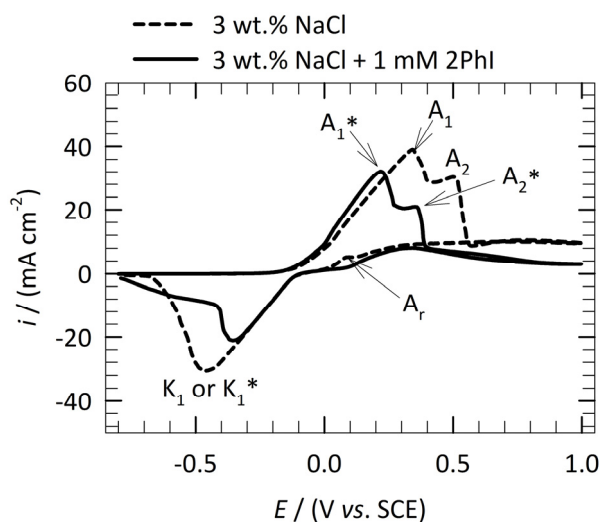


Figure 3. Cyclic voltammograms of the copper samples after 1 h of immersion in noninhibited [5] and 2PhI-inhibited 3 wt.% NaCl solution, obtained with a potential sweep rate of 20 mV s^{-1} .

Three peaks were also observed in the CV curve of the 2PhI-inhibited copper samples after 1 h of immersion in 3 wt.% NaCl solution (Figure 3). The two anodic peaks (denoted as A_1^* and A_2^*) are located at 0.217 V and 0.352 V vs. SCE, respectively, while the only cathodic peak (denoted as K_1^*) is located at -0.340 V vs. SCE . No anodic reactivation peak was detected in the CV curve of the 2PhI-inhibited copper sample. Figure 3 shows a current reduction for the first anodic peak when 2PhI is added to the 3 wt.% NaCl solution (A_1^* compared to A_1), which implies that 2PhI inhibits the formation of Cu(I). The addition of 2PhI also influences the formation of Cu(II), as seen at more positive potentials where the second anodic peak, A_2^* , is observed at lower currents compared to the respective peak of the noninhibited sample (A_2^* compared to A_2). When sweeping the potentials to even more positive values, the plateau of the 2PhI-inhibited samples is observed at lower currents compared with that of the noninhibited samples. This confirms the corrosion inhibition efficiency of 2PhI, which inhibits the oxidation of copper through the formation of a surface layer.

A current reduction was also observed in the cathodic cycle (K_1^* compared to K_1) when 2PhI was added to the chloride solution due to the high corrosion inhibition effect of 2PhI, which suppressed oxidation of Cu to Cu(I) during the anodic cycle of the CV scan.

3.3. Chronopotentiometry Measurements

Figure 4 presents the chronopotentiometry curve (E vs. t) for copper immersed in 3 wt.% NaCl solution with and without addition of 1 mM 2PhI until 100 h of immersion. EIS measurements were performed after 5, 10, 30, 50, and 100 h of immersion, in between the chronopotentiometry (resulting in a discontinuous chronopotentiometry curve at these points).

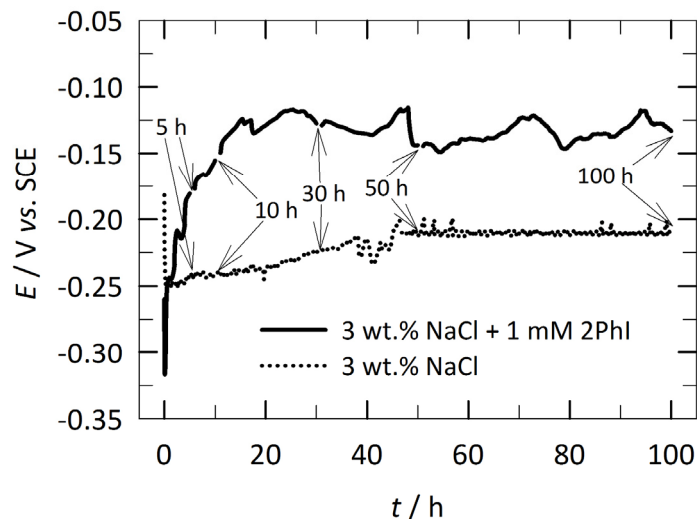


Figure 4. Chronopotentiometry curve measurements for copper samples immersed in 3 wt.% NaCl solution with and without addition of 1 mM 2PhI, at 25 °C. The times when the EIS measurements were performed (the discontinuous parts of the curve) are indicated by the arrows.

The potential of the copper samples increased after immersion in 3 wt.% NaCl solution containing 1 mM 2PhI until approx. 20 h of immersion. After 20 h of immersion the potential did not change significantly for up to 100 h. The last potential measured (at 100 h) was -0.133 V vs. SCE. Pure copper immersed in noninhibited 3 wt. % NaCl solution had the latter potential at -0.210 V vs. SCE (Figure 4). The shift to more positive potential in the presence of 2PhI suggests that the inhibitor acts predominantly as an anodic type inhibitor, which will be further investigated below by the potentiodynamic curve measurements. Similar behavior was observed also in the case of MePhI [6], under the same conditions. Moreover, no significant change was observed in the last potential measured compared to MePhI (-0.169 V vs. SCE) [6] reported previously.

3.4. Electrochemical Impedance Spectroscopy (EIS) Measurements

The EIS spectra (Nyquist and Bode plots) of the copper samples after 5, 10, 30, 50, and 100 h immersion in 3 wt.% NaCl solution containing 1 mM 2PhI are presented in Figure 5. Three distinct segments are observed in the high, middle, and low-frequency regions of the Bode plots (Figure 5b,c). A typical resistive behavior (corresponding to an uncompensated resistance, R_{Ω}) is observed in the high-frequency region (Figure 5b,c). Furthermore, in the middle frequency region typical capacitive behavior is observed as the slope of the curve is close to -1 in Figure 5b and the phase angle approaches -90° in Figure 5c. Finally, the absence of a horizontal amplitude in the low-frequency region of the modulus Bode plots (Figure 5b) is an indication of diffusion and/or adsorption/desorption processes [19,20]. A more detailed explanation of each of the above-mentioned segments and the respective behaviors has been reported previously [5–9].

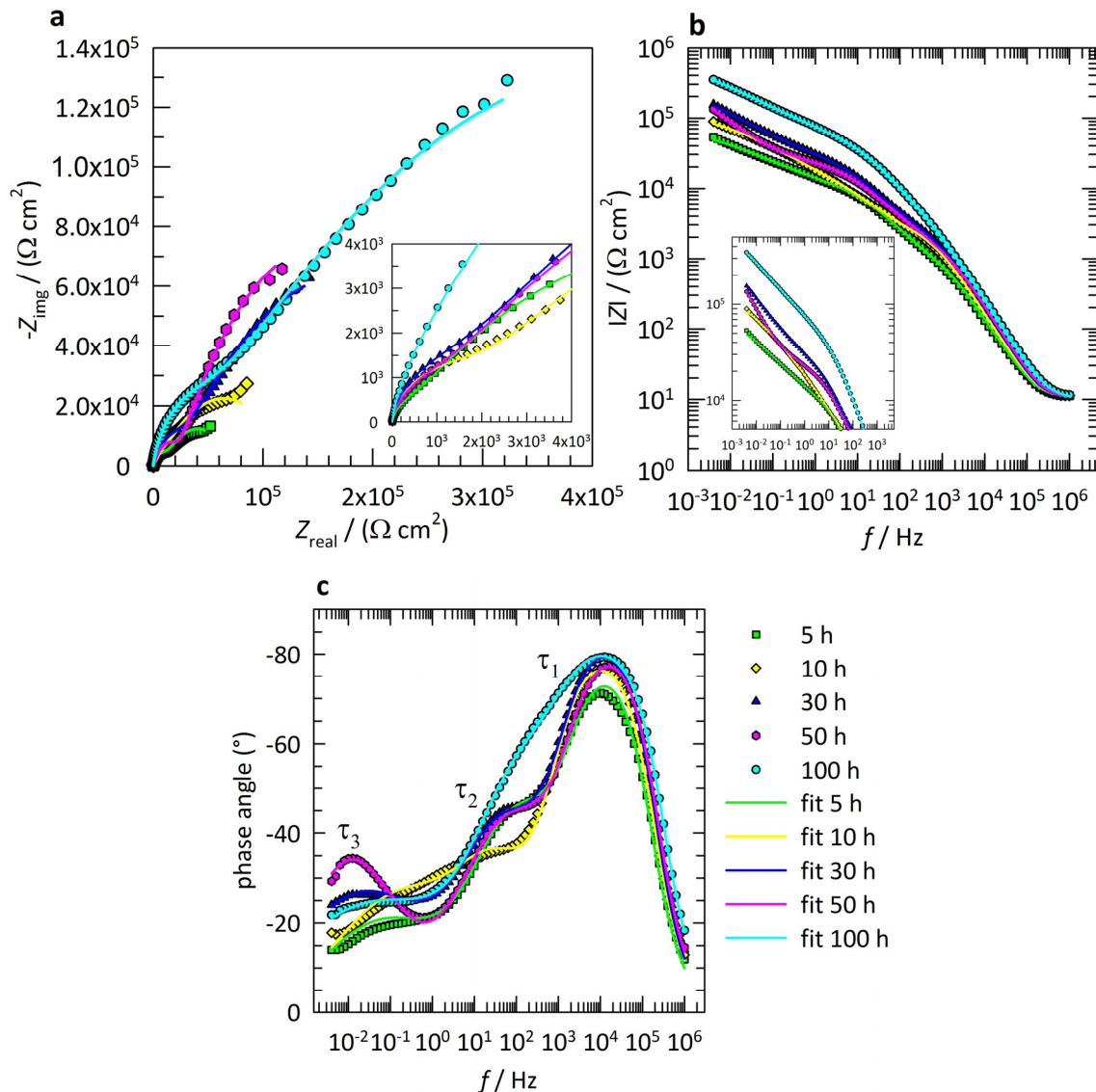


Figure 5. (a) Nyquist and (b,c) Bode plots of the copper samples after 5, 10, 30, 50, and 100 h of immersion in 3 wt.% NaCl solution containing 1 mM 2PhI. The measured EIS response is given in dotted symbols, while a solid line is used for the fitted results.

Based on the general appearance of the EIS spectra as explained above, three relaxation processes were simulated in the fitting procedure. The relaxation processes are designated as the respective τ in the phase Bode plot (Figure 5c). Moreover, various possible equivalent electrical circuit (EEC) models were used to fit the EIS measurements. However, the nested $R_{\Omega}(Q_1(R_1(Q_2(R_2(Q_3R_3))))))$ EEC model shown in Figure 6 gave the best goodness of fit, i.e., the lowest χ^2 . In the selected model (Figure 6) the uncompensated resistance, R_{Ω} (the main contribution of which comes from the solution resistance), is connected in series with resistance (R) and capacitance (Q) elements. The nonideal capacitance, Q , describes the constant phase element (CPE) with the impedance given in Equation (2) [21].

$$Z(\text{CPE}) = (Q(j\omega)^n)^{-1} \quad (2)$$

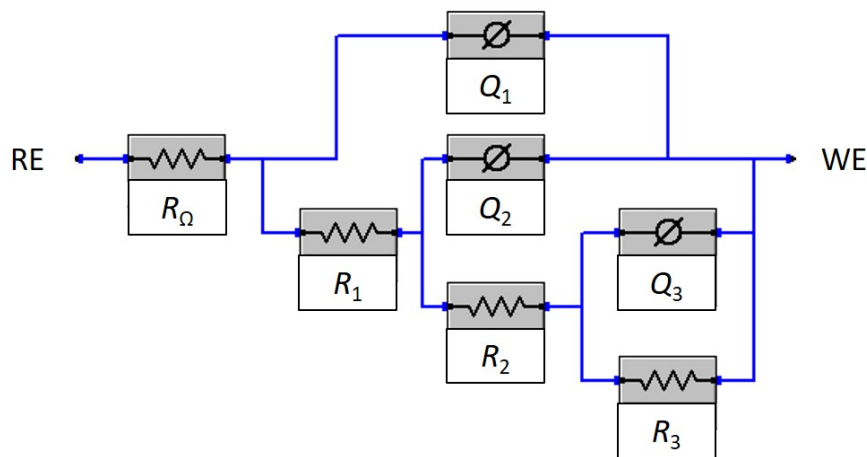


Figure 6. The nested $R_{\Omega}(Q_1(R_1(Q_2(R_2(Q_3R_3))))))$ EEC model used to fit EIS data.

Depending on the value of n , the CPE describes different behaviors, such as an ideal capacitor for $n = 1$, unrestricted diffusion for $n = 0.5$, and the distribution of the dielectric relaxation times in frequency space for $0.5 < n < 1$ [21].

The surface layer, consisting of the Cu_2O oxide layer and the adsorbed 2PhI on the copper surface, is explained by the first relaxation process R_1Q_1 . The relaxation processes were calculated as $\tau = 1/(2\pi RC)$ using the respective R and C and their approximate frequency regions are designated in Figure 5c. The first relaxation process was calculated to be in the high-frequency region, at 0.4–1.1 kHz. The second relaxation process, R_2Q_2 , calculated to be approximately 5.5–17.0 Hz, is related to the double-layer capacitance and the charge-transfer resistance from the reaction occurring at the copper/solution interface. Finally, the third relaxation process R_3Q_3 , calculated to be in the mHz region, describes the diffusion process since n is close to 0.5 [21] (Table 1).

Table 1. Fitted EIS parameters for the copper samples after 5, 10, 30, 50, and 100 h of immersion in 3 wt.% NaCl solution containing 1 mM 2PhI, obtained using the $R_{\Omega}(Q_1(R_1(Q_2(R_2(Q_3R_3))))))$ EEC model in Figure 6. Units: χ^2 ($\times 10^{-3}$), R_{Ω} ($\Omega \text{ cm}^2$), R_1 , R_2 , and R_3 ($\text{k}\Omega \text{ cm}^2$), and Q ($\mu\text{S cm}^{-2} \text{ s}^n$).

Immersion Time (h)	χ^2	R_{Ω}	n_1	R_1	Q_1	n_2	R_2	Q_2	n_3	R_3	Q_3
5	1.06	10.78	0.93	1.08	0.25	0.67	10.86	4.79	0.47	59.98	67.45
10	0.68	10.56	0.93	2.34	0.21	0.66	13.74	6.91	0.47	105.10	32.00
30	0.16	10.74	0.97	2.30	0.12	0.65	28.09	3.57	0.48	308.70	30.56
50	0.16	10.54	0.95	1.69	0.12	0.64	24.13	4.17	0.62	275.70	61.95
100	0.16	10.28	0.94	5.07	0.12	0.64	48.78	1.01	0.41	785.30	9.94

Table 1 presents the values of the parameters obtained from the fitting procedure (the model in Figure 6 was employed) of the EIS response for the copper samples after 5, 10, 30, 50, and 100 h of immersion in 3 wt.% NaCl solution containing 1 mM 2PhI. The capacitance values for the first two relaxation processes (C_{sl} and C_{dl}) were calculated based on the corresponding Q values (Q_1 and Q_2) according to Equation (3). The third relaxation process describes diffusion (n is close to 0.5), as seen in Table 1, and therefore the calculation of the capacitance is not relevant.

$$C_x = \frac{(R_x Q_x)^{1/n_x}}{R_x} \quad (3)$$

The variation of the capacitance (C_{sl} and C_{dl}) with the immersion time for the copper samples immersed for 5, 10, 30, 50, and 100 h in 3 wt. % NaCl solution containing 1 mM 2PhI is presented in Figure 7a.

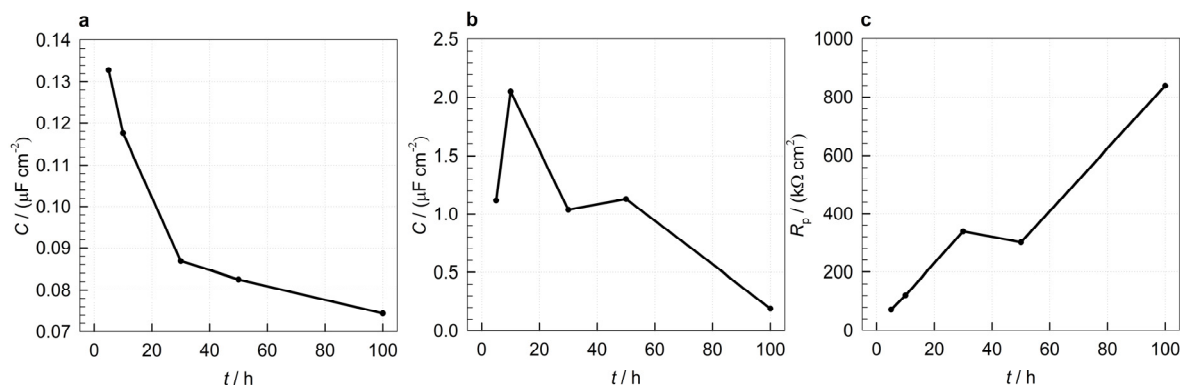


Figure 7. Variation with time of the EIS fitted results obtained using the $R_{\Omega}(Q_1(R_1(Q_2(R_2(Q_3R_3))))))$ EEC model: (a) surface layer capacitance (C_{sl}) and (b) double layer capacitance (C_{dl}) calculated according to Equation (3) and (c) polarization resistance ($R_p = R_1 + R_2 + R_3$).

The C_{sl} decreases with the increase of the surface layer thickness [22]. A decrease in the surface layer capacitance, C_{sl} (Figure 7a), was observed with increasing immersion time, which implies that a thicker surface layer formed due to the adsorption of 2PhI. The double-layer capacitance, C_{dl} , increased from 5 h to 10 h of immersion, while a decrease thereof was observed with a further increase in immersion time (Figure 7b). It was reported previously [22] that the lower the active part of the surface area (the surface not covered by the corrosion inhibitor and/or oxide), the lower the C_{dl} . In this case, the active part of the surface area decreased with increasing immersion time due to the adsorption of 2PhI on the copper surface.

Figure 7c presents the influence of the immersion time on the polarization resistance, R_p (calculated as $R_p = R_1 + R_2 + R_3$), of the copper samples immersed for 5, 10, 30, 50, and 100 h in 3 wt.% NaCl solution containing 1 mM 2PhI. The R_p increased with increasing immersion time (a nonsignificant decrease was observed at 50 h immersion). R_p is a measure of how a metallic material resists transferring electrons to electroactive species in solution; the higher it is, the more resistant it is the material. The increase in the R_p value implies that the copper samples are less susceptible (more resistant) to corrosion with the addition of 1 mM 2PhI, which confirms the latter's corrosion inhibition efficiency. Moreover, the polarization resistance of the 2PhI-inhibited copper samples increased about 2–3 orders of magnitude compared with the noninhibited samples reported previously [9].

3.5. Potentiodynamic Curve Measurements

The potentiodynamic curves measured for the copper samples immersed for 100 h in 3 wt.% NaCl solution containing 1 mM 2PhI is presented in Figure 8. The potentiodynamic curve of the noninhibited samples, presented before [11], is also given for comparison. The potentiodynamic curve measurements were started at -0.250 V vs. E_{oc} . At these potentials the cathodic polarization behavior of the copper samples is influenced primarily by the hydrogen evolution [19]. When sweeping the potential in the anodic direction, closer to E_{corr} , the mass-transport-controlled reduction of dissolved oxygen plays an important role. Tromans and Sun [23] suggested that above E_{corr} copper in chloride media dissolves at active potentials and no copper oxides are formed. As described in Section 3.2, at more positive potentials the dissolution of copper is under mixed control. On one hand, the electrodisolution of copper to form CuCl_{ads} and then the formation of the CuCl_2^- soluble complex occur. The formed CuCl_2^- , on the other hand, diffuses from the outer Helmholtz plane into the bulk solution [23,24].

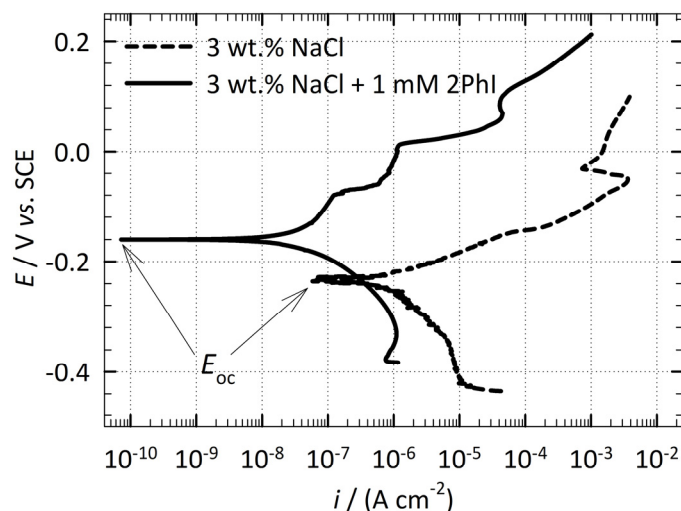


Figure 8. Potentiodynamic curve of the copper samples after 100 h of immersion in noninhibited [11] and 2PhI-inhibited 3 wt.% NaCl solutions.

As seen in Figure 8, the E_{oc} of the copper was transferred to more positive potentials in the presence of 1 mM 2PhI. The same conclusion, i.e., that the addition of 2PhI renders the system nobler, was also reached from the chronopotentiometry measurements (Section 3.3). In addition, both the anodic and cathodic branches of the potentiodynamic curve for the 2PhI-inhibited copper samples are shifted to lower current densities compared with the noninhibited potentiodynamic curve. However, the decrease in the current density of the anodic branch is more pronounced compared with the cathodic branch. In fact, the anodic branch is transferred to about three orders of magnitude lower current density with the addition of 1 mM 2PhI to the 3 wt.% NaCl solution. All these findings lead to the conclusion that 2PhI acts as a mixed-type inhibitor with a main effect on the anodic reaction of the corrosion couple. A decrease of the current density (i_{corr}) of the 2PhI-inhibited samples of more than one order of magnitude compared with the noninhibited samples was observed (Figure 8). This confirms once more the corrosion inhibition efficiency of 2PhI for copper in 3 wt.% NaCl solution.

3.6. Surface Characterization

The surface behavior of the copper samples immersed in 3 wt.% NaCl solutions with and without the addition of 1 mM 2PhI was analyzed using ATR-FTIR, contact angle measurements, 3D-profilometry, and FE-SEM analysis. Although the same sample treatment procedure was employed for all of the tests in order to allow a comparison of the results with the electrochemical measurements, two different immersion times were used. The contact angle measurements and the ATR-FTIR analysis were performed on copper samples after 1 h of immersion. After this time it is possible to analyze only the first few layers of the adsorbed inhibitor, avoiding in this way the formation of crystallites of the inhibitor on the copper surface, which do not influence the corrosion inhibition action of the adsorbed compound [13].

In order to be able to obtain more corrosion-related data in the specific environment and to test in this way the corrosion inhibition efficiency of 2PhI, a significantly longer time of immersion (31 days) was employed. The topography and the morphology of the copper samples immersed for 31 days in 3 wt.% NaCl solution with and without the addition of 1 mM 2PhI were investigated using 3D-profilometry and FE-SEM analysis.

3.6.1. Attenuated Total Reflectance Fourier Transform Infrared (ATR-FTIR) Measurements

Figure 9 compares the ATR-FTIR spectrum of the 2PhI-inhibited copper samples with the spectrum of the noninhibited copper samples, reported previously [5]. In both spectra, no broad band between

2600 and 3400 cm^{-1} related to hydrogen-bonded hydroxyl groups was observed. High amount of water molecules did not stay on the surface after the drying procedure [25]. The two peaks at 2360 and 2336 cm^{-1} , observed for both the inhibited and noninhibited copper samples, can be ascribed to the asymmetric stretching of CO_2 [26].

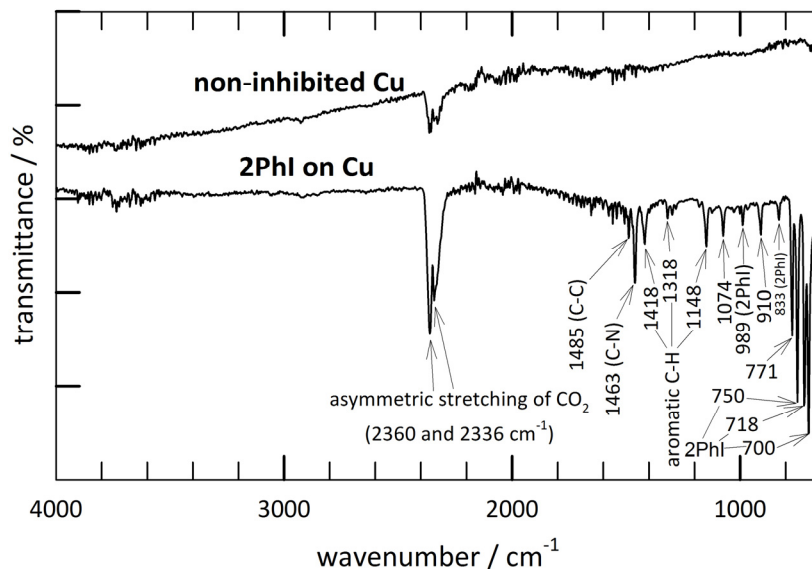


Figure 9. ATR-FTIR spectra of the 2PhI-inhibited and noninhibited [5] copper samples after 1 h of immersion in 3 wt.% NaCl solution.

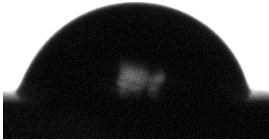
In addition, several specific peaks related to the adsorption of 2PhI on the copper surface were identified. The presence of the phenyl group was confirmed by various peaks, including the C–C stretching vibrations (at 1074 and 1485 cm^{-1}) [27], and the aromatic C–H in-plane bending modes (at 1318 and 1148 cm^{-1}) [28,29]. Sudha et al. [28] reported that the C–H in-plane bending modes of imidazole can be connected with the C=N and C–C stretching modes. Moreover, it was previously reported that the aromatic C–H out-of-plane bending modes for similar compounds are found in the range 1000–600 cm^{-1} [28–32]. In the case of 2PhI, these modes were identified at 989, 833, 771, 750, 718, and 700 cm^{-1} . The peak at 910 cm^{-1} can be attributed to the C–C–C in-plane bending modes [28]. Güllüoğlu et al. [33] attributed the peak at 1463 cm^{-1} to C–N stretching vibrations.

On that basis, we can conclude that 2PhI adsorbed on the surface, which is a requirement to be considered a corrosion inhibitor.

3.6.2. Contact Angle Measurements

Table 2 presents the average contact angle values and the respective drop shapes on the copper samples immersed for 1 h in 3 wt.% NaCl solution containing 1 mM 2PhI. In addition, the previously reported results regarding the noninhibited samples [6] are also given for comparison (Table 2). The 95% confidence interval, calculated as $\pm ts/\sqrt{N}$, (t —Student's distribution, s —standard deviation, N —number of measurements) [14], for both samples is also reported in Table 2.

Table 2. The average contact angle values (with the respective 95% confidence intervals [14]) and the drop shapes for the copper samples immersed for 1 h in noninhibited [6] and 2PhI-inhibited 3 wt.% NaCl solutions at 25 °C.

Sample Description	Average Contact Angle and Confidence Interval	Figure of the Drop Shapes on the Surface of the Samples
Ground copper sample immersed for 1 h in 3 wt.% NaCl solution	$43.0^\circ \pm 4.4^\circ$	
Ground copper sample immersed for 1 h in 3 wt.% NaCl solution containing 1 mM 2PhI	$76.0^\circ \pm 4.3^\circ$	

As seen by the contact angle values (and the drop shapes), a more hydrophobic sample was obtained when immersed in 3 wt.% NaCl solution containing 1 mM 2PhI ($\Theta = 76.0^\circ \pm 4.3^\circ$) compared to the noninhibited sample ($\Theta = 43.0^\circ \pm 4.4^\circ$) [6]. Moreover, under the same conditions, the increase in the hydrophobic nature of the 2PhI-inhibited copper samples was slightly higher compared to the MePhI-inhibited samples ($\Theta = 68.7^\circ \pm 2.9^\circ$) reported previously [6]. The slight reduction in the hydrophobic nature of the copper samples inhibited with MePhI (the addition of a $-\text{CH}_3$ group in the 2PhI structure) compared with 2PhI might be related to the orientation of the inhibitor's molecule on the surface of the copper samples (most likely the more densely packed stack of molecules with phenyl groups oriented closer to the surface and the imidazole ring closer to the substrate).

3.6.3. 3D-Profilometry Measurements

The representative 3D-profiles of the copper samples immersed for 31 days in 3 wt.% NaCl solution, with and without the addition of 1 mM 2PhI, are presented in Figure 10. A significant decrease in the surface roughness was observed with the adsorption of 2PhI. The absence of pitting formation on the inhibited copper samples is an indication that general corrosion is the predominant type of corrosion even after a relatively long immersion time.

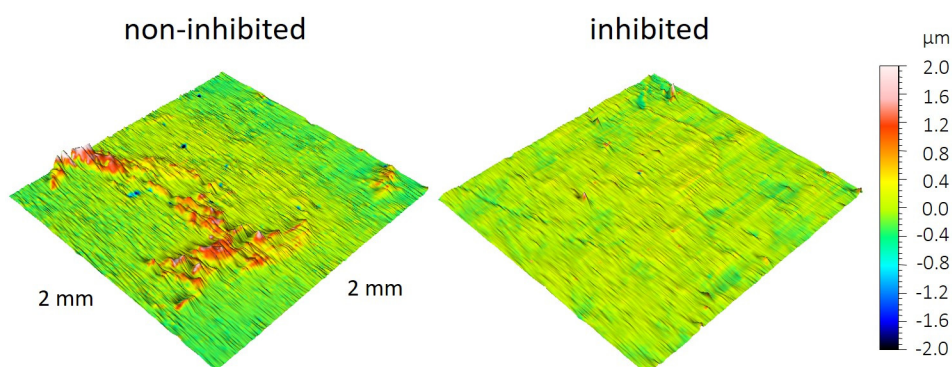


Figure 10. 3D-profiles of the noninhibited and 2PhI-inhibited copper samples after 31 days of immersion in 3 wt.% NaCl solution.

At least three replicate measurements were performed for each system and the average mean surface roughness, S_a [9], was calculated. The calculated average S_a of the copper samples immersed for 31 days in 3 wt.% NaCl solution containing 1 mM 2PhI was $0.130 \mu\text{m}$. It was previously reported [5] that the S_a of noninhibited copper samples after 31 days of immersion was $0.855 \mu\text{m}$ (S_a before immersion was $0.008 \mu\text{m}$). The S_a is directly connected to the corrosion resistance of the metal in

a specific corrosive environment. A higher S_a value implies that the metal is more susceptible to corrosion [9]. Therefore, the significant decrease in the S_a values of the copper samples with the adsorption of 2PhI further proves its corrosion inhibition efficiency.

3.6.4. Field Emission Scanning Electron Microscopy (FE-SEM) Analysis

Figure 11a–c shows SEM micrographs measured on copper samples after 31 days of immersion in 3 wt.% NaCl solution containing 1 mM 2PhI. It must be emphasized that the sample surfaces were examined in detail and representative SEM figures are given in Figure 11a–c. The main conclusion from this kind of analysis is that no significant corrosion damage was found, neither general corrosion nor pitting corrosion, thus confirming the 3D-profilometry measurements given above.

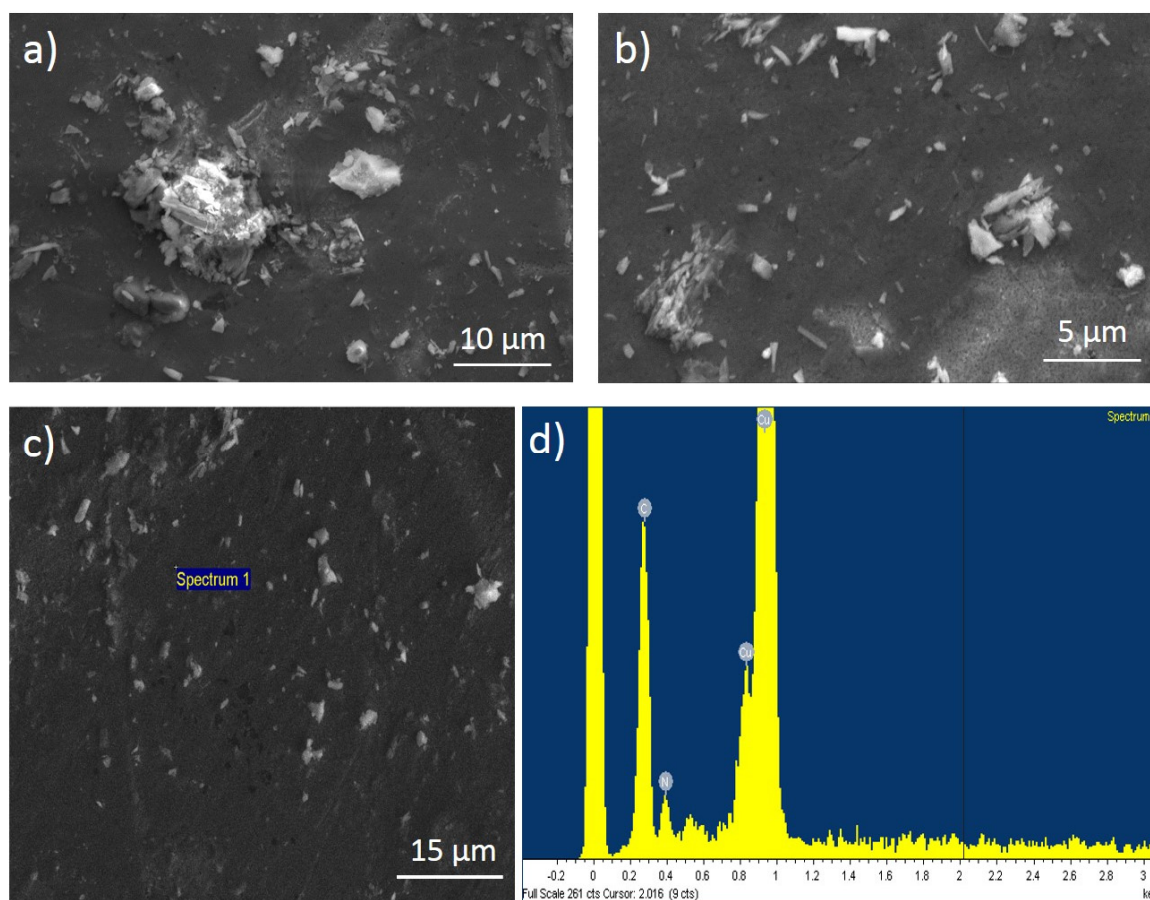


Figure 11. FE-SEM micrographs in (a–d) the EDXS spectrum for the analysis of the spot designated in (c) of the 2PhI-inhibited copper samples measured after 31 days of immersion in 3 wt. % NaCl solution.

Energy-dispersive X-ray spectroscopy (EDXS) analysis (Figure 11d) performed on the noncorroded spot of the surface designated in Figure 11c as Spectrum 1 further showed that the atomic ratio of C:N is close to 4. This ratio is close to the stoichiometric ratio of these elements in the 2PhI molecule (the exact ratio should be 4.5). This result supports the above given statement that 2PhI was adsorbed on the copper surface.

Based on the above-mentioned analyses, we can conclude that the methyl group at position 4 in MePhI (Figure 1) plays no role in the adsorption process and consequently in the corrosion inhibition process. However, the methyl group also does not interfere with the adsorption process, as MePhI was previously found to be an effective corrosion inhibitor [6,13].

4. Conclusions

Herein, various analytical techniques were employed to show for the first time that 2-phenylimidazole (2PhI) can act as an effective corrosion inhibitor for any metallic material. In this work, the metal under investigation was pure copper immersed in 3 wt.% NaCl solution.

Cyclic voltammetry measurements showed that 2PhI inhibits the oxidation of Cu to Cu(I) as well as the oxidation of Cu(I) to Cu(II). Moreover, it was proven that 2PhI acts as a mixed-type inhibitor and that it primarily inhibits the anodic reaction of the corrosion couple. Electrochemical impedance spectroscopy showed that copper corrosion in 2PhI-inhibited solution follows kinetic- and diffusion-controlled processes. The thickness of the inhibitor layer increased with time. Moreover, the addition of 2PhI rendered the copper samples more resistant to corrosion even after relatively long immersion times.

The adsorption of 2PhI was confirmed by attenuated total reflectance Fourier transform infrared spectroscopy and energy dispersive X-ray spectroscopy analysis. It was also shown that no significant pitting corrosion occurs after 31 days of immersion for the 2PhI-inhibited copper samples. Moreover, the adsorption of 2PhI significantly reduced the surface roughness of the samples, as confirmed by 3D-profilometry and scanning electron microscopy analysis. Finally, contact angle measurements showed an increase in the hydrophobic nature of the 2PhI-inhibited sample compared with the noninhibited sample.

Author Contributions: Conceptualization, M.F.; Methodology, M.F. and K.X.; Software, M.F.; Validation, M.F.; Formal Analysis, M.F. and K.X.; Investigation, M.F. and K.X.; Resources, M.F.; Data Curation, M.F. and K.X.; Writing—Original Draft Preparation, K.X. and M.F.; Writing—Review & Editing, M.F. and K.X.; Visualization, M.F. and K.X.; Supervision, M.F.; Project Administration, M.F.; Funding Acquisition, M.F.

Funding: This research was funded by the Slovenian Research Agency (BI-HR/16-17-046 and P2-0032).

Conflicts of Interest: The authors declare no conflict of interest.

References

1. Koch, G.H.; Brongers, M.P.H.; Thompson, N.G. *Corrosion Cost and Preventive Strategies in the United States*; NACE International: Houston, TX, USA, 2014.
2. Revie, R.W.; Uhlig, H.H. *Corrosion and Corrosion Control: An Introduction to Corrosion Science and Engineering*, 4th ed.; John Wiley & Sons Inc.: Hoboken, NJ, USA, 2008.
3. McCafferty, E. *Introduction to Corrosion Science*; Springer Science+Business Media, LLC: New York, NY, USA, 2010.
4. Ahmad, Z. *Principles of Corrosion Engineering and Corrosion Control*, 1st ed.; Butterworth-Heinemann: Oxford, UK, 2006.
5. Khanari, K.; Finsgar, M. The first electrochemical and surface analysis of 2-aminobenzimidazole as a corrosion inhibitor for copper in chloride solution. *New J. Chem.* **2017**, *41*, 7151–7161. [[CrossRef](#)]
6. Finšgar, M. Electrochemical analysis of 4-methyl-2-phenyl-imidazole adsorbed on Cu. *Int. J. Electrochem. Sci.* **2016**, *11*, 6775–6790. [[CrossRef](#)]
7. Finšgar, M.; Kek Merl, D. 2-mercaptobenzoxazole as a copper corrosion inhibitor in chloride solution: Electrochemistry, 3D-profilometry, and XPS surface analysis. *Corros. Sci.* **2014**, *80*, 82–95. [[CrossRef](#)]
8. Finšgar, M.; Kek Merl, D. An electrochemical, long-term immersion, and XPS study of 2-mercaptobenzothiazole as a copper corrosion inhibitor in chloride solution. *Corros. Sci.* **2014**, *83*, 164–175. [[CrossRef](#)]
9. Finšgar, M. 2-mercaptobenzimidazole as a copper corrosion inhibitor: Part I. Long-term immersion, 3D-profilometry, and electrochemistry. *Corros. Sci.* **2013**, *72*, 82–89. [[CrossRef](#)]
10. Finšgar, M.; Milošev, I. Corrosion study of copper in the presence of benzotriazole and its hydroxy derivative. *Mater. Corros.* **2011**, *62*, 956–966. [[CrossRef](#)]
11. Finšgar, M.; Lesar, A.; Kokalj, A.; Milošev, I. A comparative electrochemical and quantum chemical calculation study of BTAH and BTAOH as copper corrosion inhibitors in near neutral chloride solution. *Electrochim. Acta* **2008**, *53*, 8287–8297. [[CrossRef](#)]

12. Finšgar, M.; Milošev, I.; Pihlar, B. Inhibition of copper corrosion studied by electrochemical and EQCN techniques. *Acta Chim. Slov.* **2007**, *54*, 591–597.
13. Finšgar, M. The first X-ray photoelectron spectroscopy surface analysis of 4-methyl-2-phenyl-imidazole adsorbed on copper. *Anal. Methods* **2015**, *7*, 6496–6503. [[CrossRef](#)]
14. Massart, D.L.; Vandeginste, B.G.M.; Buydens, L.M.C.; Jong, S.D.; Lewi, P.J.; Smeyers-Verbeke, J. *Handbook of Chemometrics and Qualimetrics: Part A*; Elsevier: Amsterdam, The Netherlands, 1997.
15. Lee, H.P.; Nobe, K. Kinetics and mechanisms of Cu electrodisolution in chloride media. *J. Electrochem. Soc.* **1986**, *133*, 2035–2043. [[CrossRef](#)]
16. Kologo, S.; Eyraud, M.; Bonou, L.; Vacandio, F.; Massiani, Y. Voltametry and EQCM study of copper oxidation in acidic solution in presence of chloride ions. *Electrochim. Acta* **2007**, *52*, 3105–3113. [[CrossRef](#)]
17. Crousier, J.; Pardessus, L.; Crousier, J.P. Voltammetry study of copper in chloride solution. *Electrochim. Acta* **1988**, *33*, 1039–1042. [[CrossRef](#)]
18. Otmačić, H.; Telegdi, J.; Papp, K.; Stupnišek-Lisac, E. Protective properties of an inhibitor layer formed on copper in neutral chloride solution. *J. Appl. Electrochem.* **2004**, *34*, 545–550. [[CrossRef](#)]
19. Van Ingelgem, Y.; Tourwé, E.; Vereecken, J.; Hubin, A. Application of multisine impedance spectroscopy, FE-AES and FE-SEM to study the early stages of copper corrosion. *Electrochim. Acta* **2008**, *53*, 7523–7530. [[CrossRef](#)]
20. Silverman, D.C. Practical corrosion prediction using electrochemical techniques. In *Uhlig Corrosion Handbook*; Revie, R.W., Ed.; John Wiley and Sons: New York, NY, USA, 2000.
21. Raistrick, I.D.; Franceschetti, D.R.; Macdonald, J.R. *Impedance Spectroscopy Theory, Experiment and Application*, 2nd ed.; John Wiley & Sons Inc.: Hoboken, NJ, USA, 2005.
22. Kek Merl, D.; Panjan, P.; Kovač, J. Corrosion and surface study of sputtered Al–W coatings with a range of tungsten contents. *Corros. Sci.* **2013**, *69*, 359–368. [[CrossRef](#)]
23. Tromans, D.; Sun, R.H. Anodic polarization of copper in aqueous chloride/benzotriazole solutions. *J. Electrochem. Soc.* **1991**, *138*, 3235–3244. [[CrossRef](#)]
24. Bacarella, A.L.; Griess, J.C. The anodic dissolution of copper in flowing sodium chloride solutions between 25 °C and 175 °C. *J. Electrochem. Soc.* **1973**, *120*, 459–465. [[CrossRef](#)]
25. Finšgar, M. 2-mercaptobenzimidazole as a copper corrosion inhibitor: Part II. Surface analysis using X-ray photoelectron spectroscopy. *Corros. Sci.* **2013**, *72*, 90–98. [[CrossRef](#)]
26. Gerakines, P.A.; Schutte, W.A.; Greenberg, J.M.; van Dishoeck, E.F. The infrared band strengths of H₂O, CO and CO₂ in laboratory simulations of astrophysical ice mixtures. *Astron. Astrophys.* **1994**, *296*, 810–826.
27. Bellamy, L.J. *The Infrared Spectra of Complex Molecules*, 3rd ed.; Wiley: New York, NY, USA, 1975.
28. Sudha, S.; Karabacak, M.; Kurt, M.; Cinar, M.; Sundaraganesan, N. Molecular structure, vibrational spectroscopic, first-order hyperpolarizability and HOMO, LUMO studies of 2-aminobenzimidazole. *Spectrochim. Acta Part A* **2011**, *84*, 184–195. [[CrossRef](#)] [[PubMed](#)]
29. Erdogdu, Y.; Eskioğlu, B.; Güllüoğlu, M.T. Theoretical investigations on the molecular structure and vibrational spectral analysis of 4-methyl 2-phenylimidazole. *Opt. Spectrosc.* **2012**, *113*, 596–606. [[CrossRef](#)]
30. Koglin, E.; Witte, E.G.; Meier, R.J. The vibrational spectra of metabolites of methabenzthiazuron: 2-amino-benzothiazole and 2-(methylamino)benzothiazole. *Vib. Spectrosc.* **2003**, *33*, 49–61. [[CrossRef](#)]
31. Böhlig, H.; Ackermann, M.; Billes, F.; Kudra, M. Vibrational analysis of benzothiazoline-2-thione. *Spectrochim. Acta Part A* **1999**, *55*, 2635–2646. [[CrossRef](#)]
32. El-Azhary, A.A. A DFT study of the geometries and vibrational spectra of indene and some of its heterocyclic analogues, benzofuran, benzoxazole, bensothiophene, benzothiazole, indole and indazole. *Spectrochim. Acta Part A* **1999**, *55*, 2437–2446. [[CrossRef](#)]
33. Güllüoğlu, M.T.; Erdogdu, Y.; Karpagam, J.; Sundaraganesan, N.; Yurdakul, Ş. DFT, FT-Raman, FT-IR and FT-NMR studies of 4-phenylimidazole. *J. Mol. Struct.* **2011**, *990*, 14–20. [[CrossRef](#)]

